

See discussions, stats, and author profiles for this publication at: <https://www.researchgate.net/publication/231695178>

Development of Form II Crystallinity in Oriented Syndiotactic Polypropylene: Role of the trans-Planar Mesophase†

ARTICLE *in* MACROMOLECULES · AUGUST 2003

Impact Factor: 5.8 · DOI: 10.1021/ma0217579

CITATIONS

26

READS

18

3 AUTHORS:



Liberata Guadagno

Università degli Studi di Salerno

112 PUBLICATIONS **1,254** CITATIONS

SEE PROFILE



Concetta D'Aniello

Università degli Studi di Salerno

30 PUBLICATIONS **478** CITATIONS

SEE PROFILE



Carlo Naddeo

Università degli Studi di Salerno

53 PUBLICATIONS **656** CITATIONS

SEE PROFILE

Development of Form II Crystallinity in Oriented Syndiotactic Polypropylene: Role of the trans-Planar Mesophase[†]

Liberata Guadagno, Concetta D'Aniello, Carlo Naddeo, and Vittoria Vittoria*

Dipartimento di Ingegneria Chimica e Alimentare Università di Salerno, Via Ponte Don Melillo 1, 84084 Fisciano Salerno, Italia (U.E.)

Stefano Valdo Meille

Dipartimento di Chimica, Materiali ed Ingegneria Chimica "G. Natta", Politecnico di Milano Via Mancinelli 7, 20131 Milano, Italia (U.E.)

Received December 13, 2002; Revised Manuscript Received June 25, 2003

ABSTRACT: Films of syndiotactic polypropylene (sPP) elongated at room temperature up to a draw ratio $\lambda = 6$ showed the trans-planar form III with some trans-planar mesophase. Upon releasing tension, we obtained fibers with a high content of trans-planar mesophase and a small fraction of helical form II crystals. Released fibers were annealed at increasing temperatures up to 130 °C, and the polymorphic behavior was investigated by X-ray and FTIR. Between 60 and 80 °C, an increase of the helical forms I and II, both of them highly oriented, occurs, while the trans-planar mesophase practically disappears. Successive annealing at higher temperature brings further increase of both helical modifications until, around 130 °C, significant percentages of form II melt and recrystallize in form I. The unrelaxed $\lambda = 6$ fiber was also annealed at 100 °C, developing significant form II fractions along with form III and some form I. Two more sets of fibers were obtained under conditions in which the trans-planar mesophase was not present. In both cases, upon annealing at constant strain, no formation of the helical form II was observed and only a mixture of the trans-planar form III and the helical form I developed. The described observations suggest that, in oriented sPP samples, upon relaxing or annealing at temperatures below 100 °C, the pseudohexagonal trans-planar mesophase plays a mayor role as precursor for crystallization of the chiral form II. This appears consistent with recently proposed analyses of chiral crystallization of helical polymers.

Introduction

Syndiotactic polypropylene (sPP) shows a complex polymorphism based on different chain conformations and packing arrangements. Four basic crystalline forms of sPP have been described. Form I and II are characterized by chains in $(T_2G_2)_n$ helical conformation,^{1–3} whereas forms III⁴ and IV⁵ present chains in trans-planar and $(T_6G_2T_2G_2)_n$ conformations, respectively. Form I is the stable form of sPP, obtained under the most common conditions of crystallization either from the melt or from solution as single crystals.^{1,6–9} In the limit-ordered structure of this form, the chains are packed with an alternation of right-handed and left-handed helices along both axes of the orthorhombic unit cell, with $a = 14.50$ Å, $b = 11.20$ Å, and $c = 7.45$ Å. Extensive disorder in this regular arrangement is frequently observed, leading to an orthorhombic unit cell with $a = 14.50$ Å, $b = 5.60$ Å, and $c = 7.45$ Å. Form II corresponds to a C-centered structure in which the helical chains share the same chirality. It was originally obtained by stretching compression molded specimens of sPP samples of low stereoregularity^{2,3,10} at room temperature. Highly stereoregular samples synthesized with the new metallocenic catalysts, quenched from the melt to low temperatures and elongated to high draw ratios, give rise to the metastable trans-planar form III.⁴ However, also in this case, form II may result upon release of tension.¹⁰ Under these conditions, both a

cooperative crystal–crystal phase transition from modification III to the chiral form II,¹¹ and also a noncooperative melting recrystallization process¹² were proposed. Annealing fiber samples of form II or form III at temperatures higher than 100 °C yields mixtures of oriented forms I and II.²

Recently, Nakaoki et al.¹³ reported the spontaneous crystallization of the trans-planar form III, keeping sPP, after melting, in a bath at 0 °C for a long time. At variance, it was suggested that the crystalline phase in such samples, although correctly described as characterized by chains in the trans-planar conformation, should be identified as a mesophase, with smaller crystallites and lateral disorder in the packing of the trans-planar chains.^{14,15} We must note in this respect that the first account of a trans-planar sPP phase present in the literature,¹⁶ involving poorly stereoregular samples, unequivocally refers to a pseudohexagonal phase which is indeed the recently identified trans-planar mesophase. Form III⁴ is orthorhombic with $a = 5.22$ Å, $b = 11.17$ Å, and $c = 5.05$ Å (space group $P2_1cn$) and can be fairly clearly distinguished from the orthohexagonal trans-planar mesophase¹⁷ having $a = 6.02$ Å, $b = 10.42$ Å, and $c = 5.05$ Å.

In their studies on the trans-planar form obtained at 0 °C, identified as unoriented form III, Ohira et al. found that, with increasing temperature, 16% of form III is transformed into form II, whereas the remaining form III melts and recrystallizes into the more stable helical form I.¹⁸ Although a clearer picture of the polymorphic behavior of sPP is emerging, as a consequence of contributions by different authors, the conditions which induce the crystallization of the chiral form II remain

* To whom correspondence should be addressed. E-mail: vvittoria@unisa.it.

[†] This paper is dedicated to Professor Paolo Corradini and to Professor Giuseppe Allegra on the occasion of his 70th birthday.

somewhat elusive. Recently, Zhang et al.¹⁹ reported the epitaxial crystallization of a thin layer of sPP in form II on 2-quinoxalinol, favored by lattice matching involving interchain distances and the chain axis repeat distance. Rastogi et al.²⁰ showed, on the other hand, that form II can be obtained on cooling the isotropic melt at high pressure and suggested the presence of a thermodynamically stable region for form II in the pressure–temperature phase diagram of sPP.

It is worth recalling that the identification by X-ray diffraction of form II is based on the presence, along with twofold helical symmetry with a 7.45 Å fiber repeat, of a sharp reflection at $2\theta = 17.0^\circ$ (Cu K α), not present in the more stable form I. This peak, together with the presence of helical bands in the infrared spectrum^{3,21,22} or helical signals in the solid-state NMR-MAS spectrum,²³ allows the unambiguous identification of form II. However, in the case of both oriented and unoriented systems kept at 0 °C for a long time, the presence of a peak at $2\theta = 17.0^\circ$ is found to be due to the trans-planar mesophase. The fact that the only distinctive diffraction maximum of form II can also be attributed to the trans-planar mesophase complicates the structural analysis, in all the cases in which a trans-planar phase is present, as in samples kept at 0 °C or in relaxed fibers. In the last case, a careful analysis of first layer reflections can help clarify the phase identification.

In all the studies of annealed sPP fibers, either stretched or stress-relaxed, the question of the presence or absence of the trans-planar mesophase was never considered before. Indeed, we have reason to think that this phase was present in significant amounts and may plausibly have played a role in a number of instances where it was not recognized.^{2,4,10,11} This may well represent an important point, since previous papers dealing with oriented samples were published before the recognition of the trans-planar mesophase. An analysis of the structural transitions in light of the new phase information may help to clarify the complex sPP polymorphism.

The central issue we address in the present paper is the possible role of the trans-planar mesophase in the development of helical crystallinity, and specifically of form II, in oriented sPP samples. We have studied the thermally induced structural transformations of a sample drawn at room temperature and characterized by prevalent form III and some trans-planar mesophase crystallinity. We have also followed the development of helical crystallinity upon annealing fibers at constant length initially in form III, in which the trans-planar mesophase is respectively present and absent. Crystallization and thermally induced polymorphic transformations are followed by X-ray diffraction and infrared analysis to achieve a reliable structural picture. The final discussion is a contribution to rationalize factors leading to form II as opposed to form I crystallinity in sPP.

Experimental Section

Syndiotactic polypropylene was synthesized according to established procedures.²⁴ The polymer was analyzed by ¹³C NMR spectroscopy at 120 °C on an AM 250 Bruker spectrometer operating in the FT mode at 62.89 MHz, by dissolving 30 mg of sample in 0.5 mL of C₂D₂-Cl₄. Hexamethyldisiloxane was used as internal chemical shift reference. Our sample showed 91% syndiotactic pentads.

Preparation of the Drawn Samples. (1) Sample FR. Polymer powders were molded in a hot press (CARVER Inc.), at 150 °C, forming a film 0.1 mm thick, and rapidly quenched to 0 °C in an ice–water bath. The sample was kept in the cold bath for 3 days, and then it was drawn to $\lambda = 6$ (sample F) at room temperature. After 24 h, sample F was unhooked and kept at rest for a minimum of 24 h, obtaining sample FR.

(2) Sample FT9. Polymer powders were molded in a hot press, at 150 °C, forming a 0.1 mm thick film, rapidly quenched in a bath at 100 °C, and left for 1 h at this temperature. This film was stretched to a high draw ratio ($\lambda = 9$), at room temperature.

(3) Annealed Fibers. Sample FR was progressively annealed, in successive 2 h steps, at 40 °C (sample FR40), 60 °C (sample FR60), 80 °C (sample FR80), 100 °C (sample FR100), 120 °C (sample FR120), and 130 °C (sample FR130). Each sample, after 2 h at a given temperature, was analyzed, at room temperature, by X-ray diffraction and FTIR.

A different set of the relaxed and annealed FR fibers was sputtered with gold (thickness ~ 100 Å), used as semiquantitative internal reference for the evaluation of the reflection intensity after different treatments. Reflection intensities were measured after subtraction of the amorphous contribution.

(4) Sample FT9/60. Sample FT9 was annealed for 2 h at 60 °C and analyzed under tension.

(5) Sample F100. Sample F was annealed for 2 h at 100 °C and analyzed under tension.

(6) Sample FT100. Polymer powders were moulded in a hot press, at 150 °C, forming a 0.1 mm thick film, which was rapidly quenched to 100 °C in a boiling-water bath. The sample was directly drawn in the bath at 100 °C to $\lambda = 7$ and analyzed under tension.

Methods. All the fibers were drawn using a dynamic INSTRON 4301 apparatus. The deformation rate was 10 mm/min, and the initial length of the samples was 10 mm.

Fiber diffraction spectra were all recorded at room temperature, under vacuum, by means of a cylindrical camera with a radius of 57.3 mm and the X-ray beam direction perpendicular to the fiber axis (Ni-filtered Cu K α radiation). A Fuji BAS-1800 imaging plate system was used to record the diffraction patterns.

The infrared spectra were obtained in absorbance mode using a Bruker IFS66 FTIR spectrophotometer with a 2 cm^{−1} resolution (64 scans collected). The absorbances of the trans-planar conformational bands at 831, 963, and 1132 cm^{−1} and of the helical bands at 810, 977, and 1005 cm^{−1} were normalized with the absorbance of the band at 1153 cm^{−1}. Since this band overlaps with other vibrational modes, it was decomposed into different components, using a complex fitting form in which a Lorentzian and a Gaussian contribution were considered:

$$f(x) =$$

$$(1 - L)H \exp - \left[\left(\frac{x - x_0}{w} \right)^2 (4 \ln 2) \right] + L \frac{H}{4 \left(\frac{x - x_0}{w} \right)^2 + 1}$$

where x_0 is the peak position, H is the height, w is the width at half-height, and L is the Lorentzian component.

Results and Discussion

X-ray Analysis. (1) Unannealed and Annealed FR Samples. In Figure 1 we report the X-ray pattern

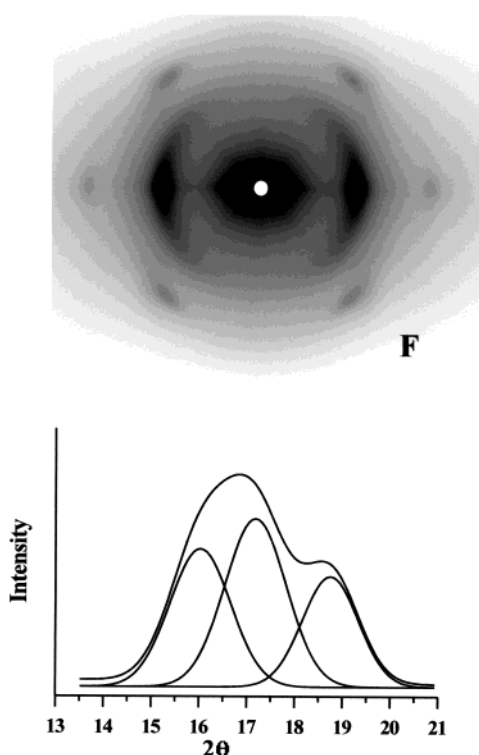


Figure 1. X-ray diffraction pattern and equatorial intensity scan of sample F.

Table 1. Shrinkage of Annealed SPP Fibers

sample	shrinkage (%)
FR	25
FR40	37
FR60	40
FR80	42
FR100	42
FR120	47
FR130	57

and the equatorial intensity scan of sample F, with fixed ends. The X-ray pattern shows, both on the equator and on the first layer, the oriented reflections of the crystalline form III described by Chatani.³ However, there is also clear evidence of the presence of significant amounts of the trans-planar mesophase, as evident in the equatorial scan. The oriented trans-planar mesophase shows a strong reflection on the equator at $2\theta = 17.0^\circ$, partially superimposed on the form III reflections. The peaks on the equator, extending in the range $14.0\text{--}21.0^\circ$ of 2θ , were resolved by performing an equatorial scan of the intensity profile and a deconvolution, clearly showing the 17° peak. We will discuss later the fact that only for very high draw ratios were we able to obtain pure form III fibers, in which there is no evidence of the 17° peak. When sample F is unhooked, it undergoes a large shrinkage, reaching a length corresponding to $\lambda = 4.5$ with respect to the initial length. A further contraction is observed on annealing the sample without mechanical constraints at increasing temperatures. Table 1 reports the shrinkage at each annealing temperature of the fibers, expressed as $(l_{\max} - l_f/l_{\max}) \times 100$, where l_{\max} is the length at full extension before the relaxation and l_f is the length after releasing tension and annealing. The shrinkage remains essentially constant for annealing temperatures from 60 to 100°C , suggesting that melting–recrystallization and major reorganization processes in this range are modest.

In Figure 2 we show the X-ray fiber diffraction patterns of samples FR, FR40, FR60, FR80, FR120, and FR130. Sample FR shows low crystallinity; the spectrum presents a broad amorphous halo at 2θ about $17.0\text{--}18.0^\circ$ that is very prominent and almost isotropic. Four reflections are apparent on the equator: The first at $2\theta = 12.3^\circ$ ($d = 7.2\text{ \AA}$) shows a small azimuthal breadth and medium-strong intensity. This reflection is observable in all the T_2G_2 helical forms and indicates that helical crystallinity was obtained on releasing the tension from the fiber F, as already described.^{25,26} The presence of helical oriented crystalline phases is also proven by the reflections on the first layer, corresponding to a fiber periodicity of 7.45 \AA . The second equatorial reflection (labeled with the arrow b) overlaps with the amorphous halo and is centered at $2\theta = 17.0^\circ$ ($d = 5.2\text{ \AA}$). A third weak and a fourth very very weak equatorial reflection are observed at $2\theta = 29.7^\circ$ and $2\theta = 34.4^\circ$, respectively, already attributed to the trans-planar mesophase.^{14–17} On the first layer, corresponding to a fiber periodicity of 7.45 \AA , we observe two reflections, namely a very weak one at $2\theta = 17.1^\circ$ ($d = 5.1\text{ \AA}$) and a highly oriented medium-strong one at $2\theta = 20.8^\circ$ ($d = 4.3\text{ \AA}$). As for the trans-planar phase, characterized by a period of 5.05 \AA , we observe the reflection at $2\theta = 23.7^\circ$ (labeled with the arrow a). Relevant observed reflections, spacings, the corresponding 2θ ($^\circ$) values, and indices for helical and trans-planar forms are listed in Table 2. The indices of the reflections of form I are given both for the traditional unit cell with $b = 5.60\text{ \AA}$ (form I^a) and for the unit cell with doubled b (form I^b).

We observe that in the FR fiber the crystalline regions coexist with a substantial amount of amorphous phase and that the ordered phase is characterized by a mixture of crystalline helical form and trans-planar mesophase. The crystalline helical modification is form II, as indicated by the presence of the 110 reflection at $2\theta = 17.0^\circ$ and the absence of the reflection at $2\theta = 16.0^\circ$, indexed for form I^a as 010. It is worth noting that the equatorial maximum at $2\theta = 17.0^\circ$ is due to the overlapping of the 110 reflection (form II) and the more intense equatorial reflection of the trans-planar mesophase.

The diffraction pattern of sample FR40 is very similar to the one just discussed. The intensities of the reflections corresponding to the helical crystals are slightly increased with respect to those of the trans-planar mesophase.

At variance, the spectrum of sample FR60 is clearly different. Both the crystallinity and the crystallite size of the helical modifications are strongly improved by annealing. The intensity of the reflection (labeled with the arrow a) on the first layer, characterized by a 5.05 \AA period, is much weaker than that of the corresponding reflection in the FR and FR40 samples. Moreover, the equatorial reflection at $2\theta = 17.0^\circ$ has a much smaller azimuthal spread. Two important features should be considered for sample FR60. First, on the equator a strong reflection (labeled with the arrow c) at $2\theta = 16.0^\circ$ appears. This reflection is observed in all the helical forms, with the exception of form II. Second, new reflections at $2\theta = 14.4^\circ$, 18.9° , 27.3° , and so forth appear on the first layer of the helical crystalline modifications. The helical 002 reflection on the meridian becomes much more intense while new reflections and some streaking become discernible on the

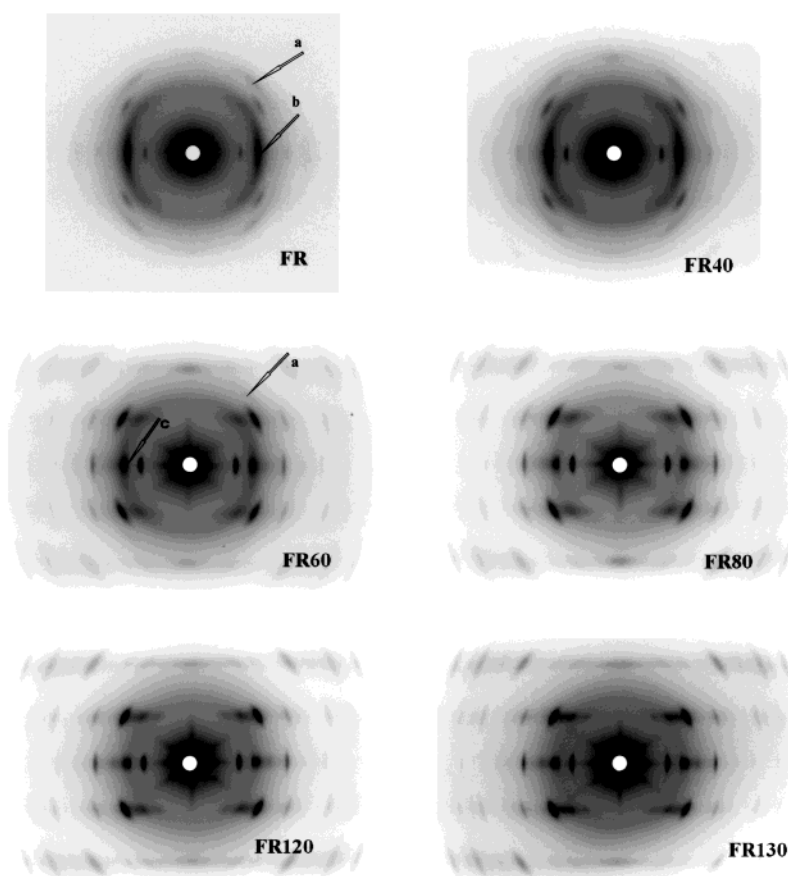


Figure 2. X-ray diffraction patterns of FR, FR40, FR60, FR80, and FR130 samples.

Table 2. Reflections Observed in the X-ray Fibers' Diffraction Spectra

2θ (deg Cu)	d (Å)	hkl (crystalline form where the reflection is allowed)	FR (I)	FR60 (I)	FR80 (I)	FR130 (I)
12.3	7.2	200 forms I ^a , I ^b , II	ms	vs	vs	vs
16.0	5.5	010 form I ^a , 020 form I ^b		s	s	s
17.0	5.2	110 form II, 110–020 orthohexagonal lattice	vs	s	s ^a	s ^a
20.1	4.4	210 form I ^a , 220 form I ^b			vw	w
24.8	3.6	400 form I ^a , I ^b , II		s	s	s
29.7	3.0	200–130 orthohexagonal lattice	w			
34.4	2.6	220–040 orthohexagonal lattice	vvw			
17.1	5.1	201 forms I ^a , II	vvw	ms	s	ms
18.9	4.7	211 form I ^b		w	w	w
20.8	4.3	111 forms I ^a , II, 121 form I ^b	ms	vs	vs	vs
27.3	3.3	401–311 form II, 321 form I ^b		ms	ms	ms
37.3	2.4	511 forms I ^a , II, 521 form I ^b		vw	vw	w
23.7 (23.0–24.4)		101–111 orthohexagonal lattice	ms	vvw		

^a Only 110 form II.

second layer line. From the discussed diffraction data of sample FR60, reported in Table 2, we can conclude that the trans-planar mesophase is considerably reduced, although still observable, while form II now coexists with other crystalline helical modifications of the form I family.

In sample FR80, as also reported in Table 2, the reflection at $2\theta = 23.7^\circ$, corresponding to the identity period of 5.05 Å, has disappeared, indicating that, upon annealing at this temperature, the transformation of the trans-planar mesophase is complete. Therefore, the equatorial spot at $2\theta = 17.0^\circ$ for samples annealed at $T \geq 80^\circ$ must be assigned only to the form II 110 reflection. For these samples the azimuthal spread of the 110 reflection is comparable with that of the other

helical reflections. After the transformation of the trans-planar mesophase, we do not record any sample contraction due to annealing up to $\sim 120^\circ\text{C}$ (see Table 1): the samples FR80 and FR100 maintain the same length, corresponding to $\lambda = 3.5$. Shrinkage again increases for samples annealed at 120 and 130 $^\circ\text{C}$, owing to the melting–recrystallization phenomena of the crystalline helical forms.

Fibers FR100, FR120, and FR130 show the same reflections as those of the FR80 sample. Only the relative intensities vary somewhat, and the amorphous halo is further reduced. The X-ray diffraction pattern for sample FR100 is not reported here because of its similarity with that of sample FR120. Data for sample FR130 are given in Table 2.

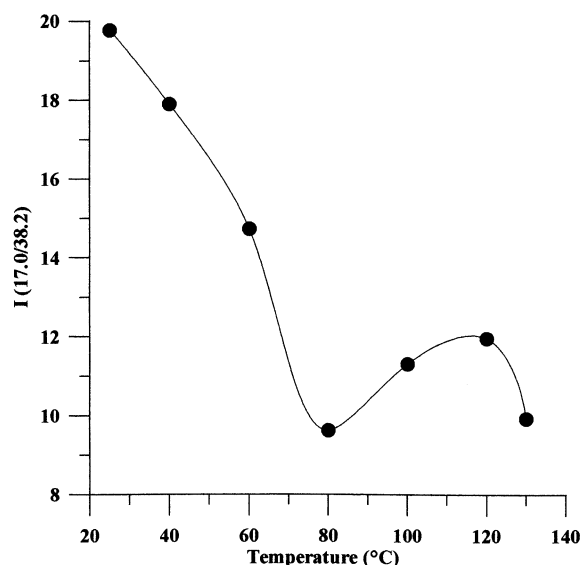


Figure 3. Intensity ratio $I_{2\theta=17.0^\circ}/I_{2\theta=38.2^\circ}$ as a function of the annealing temperature.

In the FR, FR40, and FR60 patterns the interpretation of the equatorial reflections is complicated by the superposition at $2\theta = 17.0^\circ$ of reflections due to form II and to the trans-planar mesophase. To evidence how the proportions of these two phases vary, we used as internal reference (see Experimental Section) the 111 reflection ($2\theta = 38.2^\circ$) of the gold sputtered on the samples. In Figure 3 the intensity ratio $I_{2\theta=17.0^\circ}/I_{2\theta=38.2^\circ}$ as a function of the annealing temperature is shown. The contribution of the amorphous background was subtracted in all cases. The relative intensity at $2\theta = 17.0^\circ$ decreases up to 80°C , while the trend seems reversed between 80 and 120°C , and again decreases above 120°C . Since the reflection at $2\theta = 17.0^\circ$ is observed only in form II and in the trans-planar mesophase, and also considering that all the other

helical reflections increase, we can conclude that the decrease of intensity upon annealing in the range 20 – 80°C is due to the balance between the progressive reduction of the trans-planar mesophase and the increase of form II. When the mesophase is completely transformed (as shown from the absence of the trans-planar reflection on the first layer), further development and perfecting of form II determines some increase of intensity at $2\theta = 17.0^\circ$ up to 120°C . The annealing determines further crystallization of the amorphous phase into form II, nucleated by the form II crystals already present in the sample. This is a standard crystal nucleation and growth mechanism and explains the increasing amounts of form II obtained by annealing above 80°C . At higher temperatures, melting of form II starts, giving rise to a reorganization of the fiber and recrystallization into form I^b.

In Figure 4 we report the azimuthal intensity distribution of the maximum at $2\theta = 17^\circ$, in the range from 180° to 360° of the azimuthal angle ψ , after subtraction of the amorphous background. In the patterns recorded at different temperatures, three peaks are observed: the central one, at $\psi = 270^\circ$ is the equatorial reflection, while the symmetrical lateral ones are essentially 201 form II reflections ($2\theta = 17.1^\circ$). Form I contributions to this reflection cannot be ruled out, as one of the space groups (*Pcaa*) proposed for the disordered form I also allows this reflection with a structure factor comparable to that of form II.² The intensity increase of the 201 reflections up to 120°C is correlated to the development essentially of form II helical crystallinity, but some form I contributions cannot be ruled out. Only at 130°C do we record a decrease of the relative intensity of the 201 reflections, as compared to that of sample FR120. This decrease can be attributed to recrystallization of forms I^a and II into form I^b, for which this reflection is prohibited. For the equatorial reflection, we observe that the azimuthal spread undergoes a progressive narrowing with increasing annealing temperatures, as is

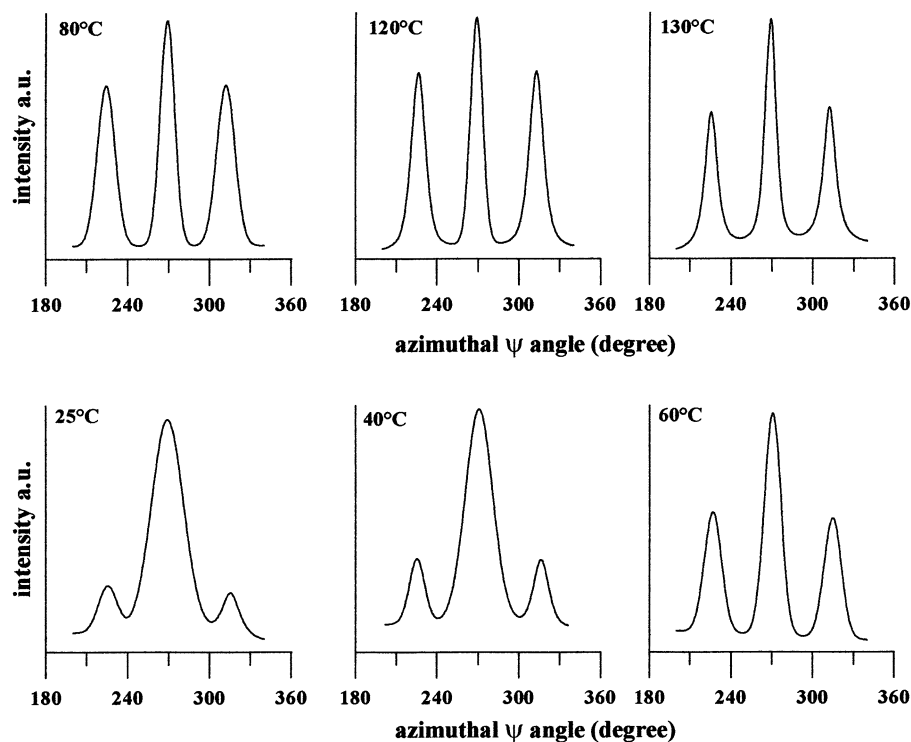


Figure 4. Azimuthal intensity distribution of the maximum at $2\theta = 17^\circ$, in the range 180° to 360° of the azimuthal angle ψ .

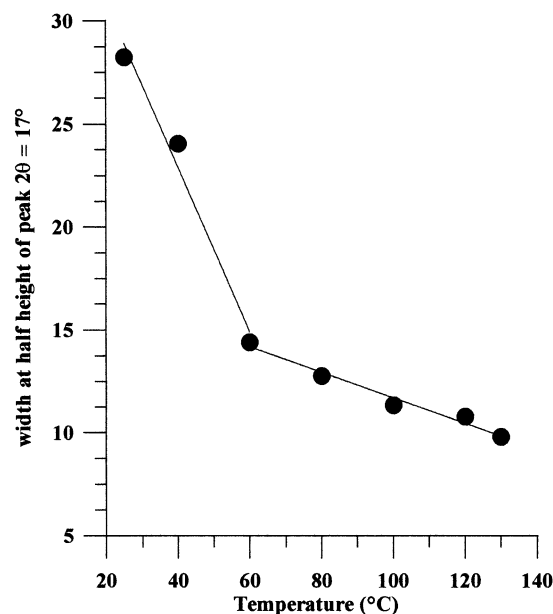


Figure 5. Azimuthal spread of the equatorial reflection at $2\theta = 17^\circ$ as a function of the annealing temperature.

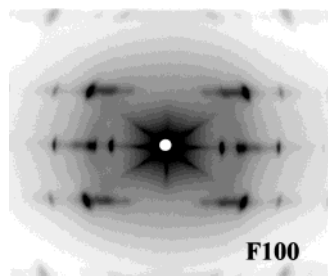


Figure 6. X-ray diffraction pattern of the F100 sample.

apparent in Figure 5. The decrease in width is very rapid in the range 20–60 °C and more gradual after 60 °C. This discontinuous behavior provides strong evidence that the annealing process does not occur through the progressive increase of the degree of orientation of the same crystalline modification. The azimuthal width behavior of the equatorial reflection, consistent with the evolution of its intensity, can be interpreted in terms of a progressive transformation of the mesophase into form II up to ~60 °C.

The diffraction data of the stretched, relaxed FR samples indicate at temperatures below 60 °C progressive crystallization into the helical form II from the trans-planar mesophase. After annealing above 60 °C, the scattering due to the mesophase is virtually absent while further crystallization proceeds in form II and, increasingly, into the thermodynamically stable form I.

(2) Samples F100, FT9/60, and FT100. The X-ray fiber diffraction patterns of samples F100, FT9, FT9/60, and FT100 are shown in Figures 6–8. The diffraction data are reported in Table 3. We recall briefly that sample F100 was obtained by annealing sample F at 100 °C at constant length, while both FT9/60 and FT100 are unrelaxed fibers obtained from films compression molded at 150 °C, crystallized at 100 °C, and stretched at room temperature and at 100 °C, respectively.

The diffraction pattern of sample F100 does not show any evidence of the trans-planar mesophase apparent in sample F, but only forms I and II. The pattern of fiber FT9, obtained by stretching to $\lambda = 9$ at room temperature, corresponds to the crystalline trans-planar form

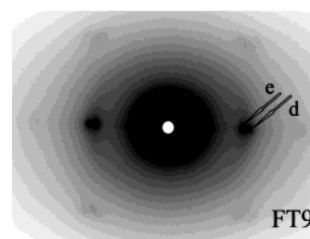
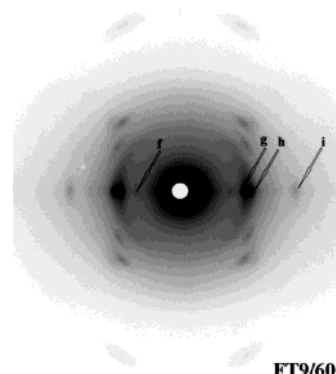
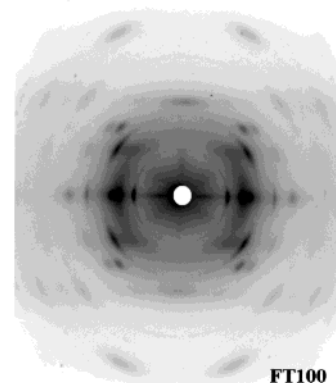


Figure 7. X-ray diffraction pattern of the FT9 sample.



FT9/60



FT100

Figure 8. X-ray diffraction patterns of the FT9/60 and FT100 samples.

III, well oriented and developed, without evidence of the trans-planar mesophase. The intense equatorial reflections 020 (arrow e) and 110 (arrow d) of form III at $2\theta = 15.9^\circ$ and 18.8° are clearly distinguishable, and no evidence of equatorial reflection at $2\theta = 17.0^\circ$ is noticed. This pattern presents noticeable differences with respect to the published form III patterns,⁴ especially in the azimuthal distribution of the strong equatorial spot centered at $2\theta \approx 17^\circ$, which is absent in the FT9 sample. When fiber FT9 is annealed at 60 °C (sample FT9/60), the pattern changes, as shown in Figure 8: on the equator, besides the form III 020 (labeled with the arrow g), 110 (arrow h), and 130 (arrow i) reflections, we observe the 200 (arrow f) and 010 (arrow g) reflections of the helical forms. To better understand the equatorial reflections, we note that the second spot (arrow g), which is wider and more intense, with respect to the third one, includes the reflection at $2\theta = 15.9^\circ$ (020-form III) and the reflection at $2\theta = 16.0^\circ$ (010-form I^a). On the first layer, corresponding to a fiber periodicity of 7.45 Å, we observe the reflection at $2\theta = 20.8^\circ$ indexed for form I^a as 111. On the layer corresponding to a

Table 3. Reflections Observed in the X-ray Fibers' Diffraction Spectra

2θ (deg Cu)	d (Å)	hkl (crystalline form where the reflection is allowed)	F100 (I)	FT9 (I)	FT9/60 (I)	FT100 (I)
12.3	7.2	200 forms I ^a , I ^b , II	vs		vw	vs
15.9	5.6	020 form III		vs	vs	vs
16.0	5.5	010 form I ^a , 020 form I ^b	s		s	vs
17.0	5.2	110 form II	s			
18.8	4.7	110 form III		vs	vs	vs
24.8	3.6	400 forms I ^a , I ^b , II	s			ms
29.7	3.0	130 form III		ms	mw	w
17.1	5.1	201 forms I ^a , II	ms			vw
18.9	4.7	211 form I ^b	ms			vw
20.8	4.3	111 forms I ^a , II, 121 form I ^b	s		ms	vs
27.3	3.3	401–311 form II, 321 form I ^b	ms			vw
23.7	3.75	021 form III		s	s	s
(23.0–24.4)						
25.8	3.46	111 form III		s	ms	ms

5.05 Å fiber periodicity, we observe instead the 021 and 111 reflections of the trans-planar form III. Sample FT9/60 therefore shows reflections of the trans-planar form III that are strong and well resolved, just as sample FT9, and in addition some reflections of the helical form I^a. The absence of the equatorial reflection at $2\theta = 17.0^\circ$ is strong evidence that, with this method of fiber preparation, form II does not develop.

In the case of sample FT100, observations similar to those for sample FT9/60 indicate that it is a mixture of helical form I^a (better developed than in sample FT9/60) and trans-planar form III. Also in this case the trans-planar mesophase is initially absent (at 100 °C) and no crystallization in form II occurs upon cooling. On the other hand, annealing at temperatures of 100 °C or higher, these samples relax and/or break. Under the circumstances, both forms I and II develop. This may be explained considering that relaxation of form III results, in part, in the formation of some amorphous and some transient trans-planar mesophases, which in turn recrystallize, giving rise to forms I and II.

Summarizing, we can state that, either annealing fibers in form III, which do not contain the trans-planar mesophase, or directly drawing at high temperatures, there is no development of form II crystallinity as long as the samples are unrelaxed. On the contrary, annealing oriented samples, both relaxed and at constant length, containing the trans-planar mesophase, gives rise to significant amounts of form II crystallinity. Form II containing systems can also be obtained by relaxing samples which contain or are able to develop a significant trans-planar mesophase component.

As already mentioned, in papers published before the recognition of the trans-planar mesophase, a transition from form III to form II was reported. However, in those supposedly pure form III samples, it seems plausible to suggest the presence of substantial amounts of the trans-planar mesophase. In fact, even for the sample used in ref 4 for the crystal structure determination of form III, some evidences suggest the presence of the trans-planar mesophase: (i) the experimental density is nearly 7% lower than that calculated for pure form III and closely similar to the one calculated for the mesophase; (ii) the azimuthal spread of the broad and very strong equatorial diffraction maximum at $\sim 17^\circ$ in the reported fiber pattern is very large as compared to the azimuthal spread of other reflections, suggesting that the mesophase may contribute; (iii) the first layer form III 021 reflection, coinciding with a mesophase diffraction maximum shows strong deviations between a weak calculated and a strong observed value, consistent with the presence of significant amounts of meso-

phase in the sample. Moreover, in the present paper we were able to obtain what we can confidently regard as pure form III, only for sample FT9 at very high draw ratios ($\lambda = 9$), not previously reported. It may be therefore plausible to suggest that the transition from form III to the helical form II, described in the literature for oriented fibers, could be more accurately described as a form III–mesophase–form II transition.

FTIR Analysis. It is important to consider IR measurements, which are very useful for providing information on the chain conformation, in conjunction with X-ray analysis. As a matter of fact, a detailed knowledge of the chain conformation provides us the opportunity to better understand the structural transformations occurring in the fibers.

In Figure 9 we report the FTIR absorbance spectra (1300–1700 cm^{-1}) of samples FR and FR130. We observe that, in sample FR, the bands of the trans-planar conformation of sPP, appearing at 831, 963, and 1132 cm^{-1} , are clear and well developed. At variance, in sample FR130, the trans-planar bands are considerably reduced, whereas all the helical bands, appearing at 810, 977, and 1005 cm^{-1} , are markedly increased. These data confirm the X-ray results. Sample FR contains a large number of chains in the trans-planar conformation, whereas only small fractions of chains in the helical conformation are present (form II). In sample FR130 there is a prevalent fraction of chains in the helical conformation, even if the bands diagnostic of the trans-planar conformation are not absent. As no reflections due to the trans-planar mesophase appear in the X-ray pattern, the trans-planar chains must reside in the amorphous component connecting the crystalline domains or in defect structures.²³ To follow the conformational transformations during annealing, we analyzed the infrared bands for all fibers. We normalized the absorbance of these bands with the absorbance (A) of the band at 1153 cm^{-1} , which is independent of the conformation, obtaining the ratio $R = A_{(\text{trans-planar})}/A_{(1153)}$. The band at 1153 cm^{-1} , which overlaps with other vibrational modes, was decomposed into different components as described in the Experimental Section.

Figure 10 shows the ratio R for the trans-planar band at 963 cm^{-1} as a function of annealing temperature. This band strongly decreases up to 80 °C and then reaches an almost constant, although not negligible, value. The other trans-planar bands, not reported here, show the same trend. From the comparison between these data and those reported in Figure 2, it is evident that the decrease between 40 and 80 °C is due to the transformation of the trans-planar mesophase.

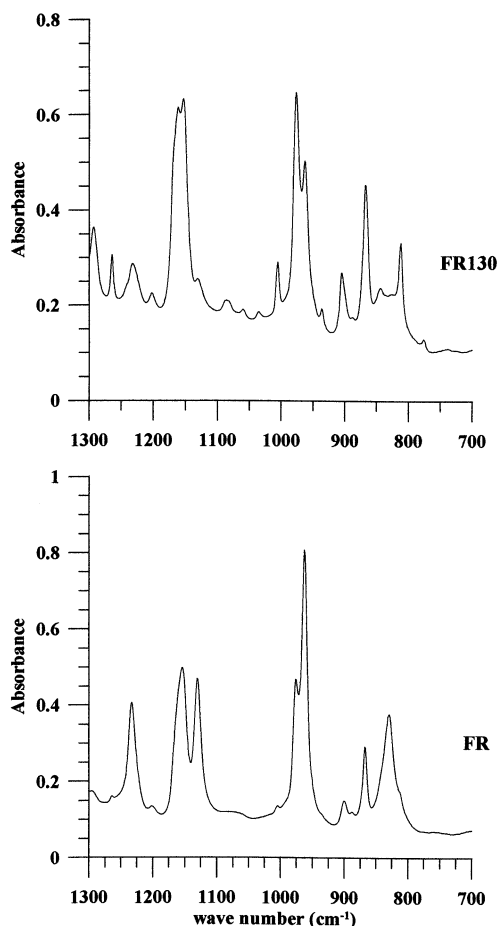


Figure 9. FTIR spectra in absorbance (1300–700 cm^{-1}) of the FR and FR130 samples.

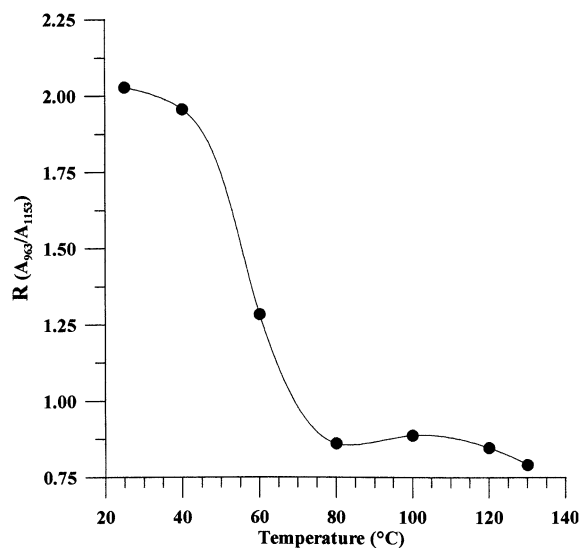


Figure 10. Ratio R for the trans-planar band at 963 cm^{-1} as a function of the annealing temperature.

The ratio R for the helical band at 812 cm^{-1} is shown in Figure 11. The trend, in this case, is opposite to the previous one, indicating that the decrease of the trans-planar sequences and the increase of the helical ones are correlated events.

As already discussed in the X-ray section, the helical modification is form II in the sample annealed at 40 $^{\circ}\text{C}$; the observed increase of the R parameter at this temperature is exclusively due to the increase of helical

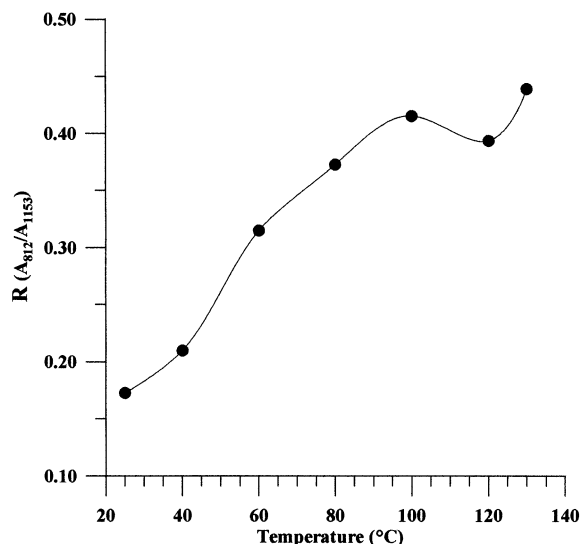


Figure 11. Ratio R for the helical band at 812 cm^{-1} as a function of the annealing temperature.

sequences that crystallize in such crystallographic modifications. Therefore, the trans-planar mesophase is converted into form II. The increase of R recorded at $T > 40$ $^{\circ}\text{C}$ is instead due to helical sequences that crystallize either in form I or in form II.

Concluding Remarks

Crystallization of sPP in form II is still not fully understood. Packing energy calculations²⁷ and experimental melting behavior support the view that, at ambient pressure, it is somewhat less stable than form I, although the two modifications share the same $(T_2G_2)_n$ helical conformation and have essentially the same density. A well recognized characteristic of form II is that, irrespective of the nonchiral nature of the sPP chain, it presents a chiral space group, implying that individual crystals are each built of isochiral helices. This arrangement seems less probable than the one found in the more stable form I crystals, where an equal number of left- and right-handed helices coexist. These considerations imply that crystallization at ambient pressure into form II rather than form I is likely to result from kinetic factors, like a greater growth rate or preferential nucleation.

Quite clearly, forms I and II show different packings: helices in the chiral form II are relatively close to a sixfold coordination while in form I a pseudotetragonal arrangement is approached. This feature corresponds to the predictions outlined in a paper on chiral crystallization of helical polymers by Allegra et al.,²⁸ implying that “closeness” to hexagonal packing of chains in crystal structures of nontrivial helical molecules (i.e. non-zigzag planar) is strongly correlated with the probability of the crystal structures being chiral, that is, adopting a chiral space group. How close polymer crystal structures are to a pseudo-hexagonal arrangement can be gauged, for example, by the hexagonality index H , which is exactly 1.00 for pseudo-hexagonal structures while values of 1.41 and 1.73 correspond respectively to tetragonal and trigonal structures. In the case of sPP, the index H is found to be 1.39 and 1.33 for the chiral forms II and IV, respectively, while it is 1.64 for racemic form I. The idea is that pseudo-hexagonal packing in the precrystallization state (nuclei, mesophases, and possibly also other crystalline phases) tends to imply, if

preserved during crystallization, adoption of isochiral helical conformations in crystals of nontrivial helical molecules. The main reason underlying this behavior is that, on a pseudo-hexagonal lattice, one single object can be packed regularly, whereas attempts to arrange two distinct objects lead unavoidably to frustration, which is usually a low energy but also a low entropy state.

In the case of sPP, there is a notable additional feature clearly resulting from experiment, namely that crystallization of chains in the achiral trans-planar conformation occurs with, or close to, a pseudo-hexagonal arrangement: the value of H for trans-planar, achiral, form III is 1.18, while it is 1.00 in the trans-planar mesophase. This suggests that pseudo-hexagonal arrangements, expected to some degree also in amorphous sPP, are likely to be particularly compatible and thus favor the trans conformation. With appropriate annealing or releasing of the stress on the samples, the trans chains will adopt the more stable helical conformation. If this occurs at low enough temperatures and rapidly enough to maintain local memory of the pseudo-hexagonal chain packing, then the chiral form II rather than form I will be likely to develop, since its packing is closer to hexagonal. On the other hand, crystallization from the melt at high temperatures, close to equilibrium conditions, allows extensive reorganization and tends to proceed to the thermodynamically stable, twofold helical, racemic form I, unless under the influence of appropriate nucleating agents.

The above framework is compatible with the development of form II proceeding either from the trans-planar mesophase or by a crystal-crystal transformation from modification III. This could well occur by a specific molecular mechanism involving cooperative generation of gauche torsions of identical sign in contiguous chains, as recently suggested.¹¹ The suggestion is interesting, although it is difficult to prove conclusively: it seems useful to give careful consideration to additional available data and consider viable alternatives, consistent with recent electron diffraction and microscopy evidence.¹² The experimental results of the present paper represent strong evidence that, in order for form II to develop, the trans-planar mesophase has to be present, at least in the case of oriented samples kept under tension. This is consistent with a role which can be played by the mesophase in the nucleation and growth of form II. It seems important to stress that in the case of the original, low stereoregularity samples, yielding quite easily form II,¹⁶ the trans phase obtained in the orientation process was certainly the mesophase, as apparent from the reflections mentioned in the original literature.¹⁶ Indeed, well organized form III was recognized only later using more stereoregular samples,⁴ but also in that case, the experimental evidence seems compatible with the presence of non-negligible amounts of the trans-planar mesophase. Even in the case of high pressure crystallization, under conditions for which form II has been proposed to be the stable form,²⁰ the reported data could in principle be compatible with a role of the trans-planar mesophase, since only unoriented diffraction data are supplied and the main reflection of the trans-planar mesophase, with a 5.2 Å spacing, coincides with the most characteristic form II reflection.

It appears quite reasonable that heating the well ordered form III at constant length will result in some

annealing and ultimately in melting at high enough temperatures. High chain mobility will cause loss of local order and plausibly recrystallization into the more stable form I. The question whether at low temperature relaxation of form III may give rise to the trans-mesophase and, through this path, to form II seems to require additional investigation. Direct crystallization of amorphous sPP into form III at high temperature seems unlikely: with high chain mobility, form I will tend to develop. Also form II, under the circumstances, is only likely to be obtained with appropriate nucleating agents¹⁹ or by self-nucleation. On the other hand, from the amorphous phase at lower temperatures, if the chain mobility is limited, mesophase domains will rather develop which, upon sufficient stretching, will give rise to form III or, by subsequent relaxation and annealing, to form II. As discussed in ref 11, crystal to crystal form II-form I or form IV-form I transitions are basically impossible, since helix inversion within crystals would be required. The role of the metastable trans-planar mesophase could therefore be central in the crystallization of sPP and in its polymorphic behavior.

Acknowledgment. This work was supported by MIUR-Italia (PRIN 2002).

References and Notes

- Lotz, B.; Lovinger, A. J.; Cais, R. E. *Macromolecules* **1988**, *21*, 2375.
- De Rosa, C.; Corradini, P. *Macromolecules* **1993**, *26*, 5711.
- Corradini, P.; Natta, G.; Ganis, P.; Temussi, P. A. *J. Polym. Sci.* **1967**, *16*, 2477.
- Chatani, Y.; Maruyama, H.; Noguchi, K.; Asanuma, T.; Shiomura, T. *J. Polym. Sci., Part C* **1990**, *28*, 393.
- Chatani, Y.; Maruyama, H.; Asanuma, T.; Shiomura, T. *J. Polym. Sci., Part B: Polym. Phys. Ed.* **1991**, *29*, 1649.
- Lovinger, A. J.; Lotz, B.; Cais, R. E. *Polymer* **1990**, *31*, 2253.
- Lovinger, A. J.; Davis, D. D.; Lotz, B. *Macromolecules* **1991**, *24*, 552.
- Lovinger, A. J.; Lotz, B.; Davis, D. D.; Padden, F. J. *Macromolecules* **1993**, *26*, 3494.
- De Rosa, C.; Auriemma, F.; Vinti, V. *Macromolecules* **1997**, *30*, 4137.
- De Rosa, C.; Auriemma, F.; Vinti, V. *Macromolecules* **1998**, *31*, 7430.
- Lotz, B.; Mathieu, C.; Thierry, A.; Lovinger, A. J.; De Rosa, C.; Ruiz De Ballestreros, O.; Auriemma, F. *Macromolecules* **1998**, *31*, 9253.
- Bonnet, M.; Yan, J.; Petermann, T.; Zhang, B.; Yang, D. *J. Mater. Sci.* **2001**, *36*, 635.
- Nakaoki, T.; Ohira, Y.; Hayashi, H. *Macromolecules* **1998**, *31*, 2705.
- Vittoria, V.; Guadagno, L.; Comotti, A.; Simonutti, R.; Auriemma, F.; De Rosa, C. *Macromolecules* **2000**, *33*, 6200.
- Loos, J.; Huckert, A.; Petermann, J. *Colloid Polym. Sci.* **1996**, *274*, 1006.
- Natta, G.; Peraldo, M.; Allegra, G. *Makromol. Chem.* **1964**, *75*, 215.
- Guadagno, L.; D'Aniello, C.; Naddeo, C.; Vittoria, V.; Meille, S. V. *Macromolecules* **2002**, *35*, 3921.
- Ohira, Y.; Horii, F.; Nakaoki, T. *Macromolecules* **2000**, *33*, 5566.
- Zhang, J.; Yang, D.; Thierry, A.; Wittmann, J. C.; Lotz, B. *Macromolecules* **2001**, *34*, 6261.
- Rastogi, S.; La Camera, D.; van der Burgt, F.; Terry, A. E.; Cheng, S. Z. D. *Macromolecules* **2001**, *34*, 7730.
- Natta, G.; Pasquon, I.; Corradini, P.; Peraldo, M.; Pegoraro, M.; Zimbelli, A. *Atti Accad. Naz. Lincei, Cl. Sci. Fis., Mat. Nat., Rend* **1960**, *28*, 539.
- Zimbelli, A.; Natta, G.; Pasquon, I. *J. Polym. Sci.* **1963**, *4*, 411.
- Sozzani, P.; Simonutti, R.; Galimberti, M. *Macromolecules* **1993**, *26*, 5782.
- Guadagno, L.; Fontanella, C.; Vittoria, V.; Longo, P. *J. Polym. Sci., Part B* **1999**, *37*, 173.

- (25) Guadagno, L.; D'Aniello, C.; Naddeo, C.; Vittoria, V. *Macromolecules* **2001**, 34, 2512.
(26) Guadagno, L.; D'Aniello, C.; Naddeo, C.; Vittoria, V. *Macromolecules* **2000**, 33, 6030.

- (27) Palmo, K.; Krimm, S. *Macromolecules* **2002**, 35, 394.
(28) Meille, S. V.; Allegra, G. *Macromolecules* **1995**, 28, 7764.
MA0217579